

Study of early soot formation from alkyl-aromatic fuels

O.Mathieu¹, N. Djebaili-Chaumeix¹, F. Douce², P. Manuelli³, C.-E. Paillard^{*, 1}

¹Centre National de la Recherche Scientifique, Institut de Combustion Aérothermique Réactivité et environnement

²TOTAL – Centre de Recherche de Solaize – Nouveaux carburants et Moteurs

³TOTAL – Direction Recherche

Abstract

The length effect of the lateral chain of alkyl-aromatic hydrocarbons on the soot tendency was investigated experimentally at high pressure using a heated shock-tube coupled with a laser beam extinction technique. The main results obtained have shown that the soot tendency, mainly soot induction delay times and soot yield, of alkyl-aromatics depends on the length of the alkyl chain. If the induction delay time increases moderately with the alkyl chain length, a strong decrease of the soot yield is observed. Concerning the evolution of the soot growth constant versus the temperature, toluene and *n*-butyl-benzene were found to exhibit a variation of k_f versus temperature similar to other aromatic compounds while for *n*-heptyl-benzene, an intermediate behavior was observed between aromatic and aliphatic compounds.

Introduction

Soot particles emissions are responsible of (i) adverse health effects [1-2], (ii) interactions with climate change [3]. However, among pollutants formed during combustion, soot is definitely the less understood despite efforts of the scientific community. In order to better understand the soot formation, in view to reduce emissions, acquisition of fundamental data concerning their inception, growth and oxidation, in well defined laboratory reactors, are needed. Shock-tube is a suitable technique to study early soot formation [4-6]. This technique gives the possibility to work with a homogenous reactor and to measure soot under defined temperature and pressure, with an observation time limited to few milliseconds.

Fossil fuels are constituted of hundreds or even thousands of different components. In order to obtain a better understanding of the phenomena, it is necessary to investigate the contribution of each component to the soot load. Mono-aromatic compounds are present in significant weight proportion in all fuels used in transports (between 6 and 54 % in gasoline [7], around 18 % in kerosene [8] and around 17 % in diesel fuel [7]). The structure (namely length, number and nature of the lateral chain) of these mono-aromatic compounds is dependant on the temperature range of distillation and refining conditions; and, hence, on the fuel.

Specific Objectives

The purpose of this paper is to evaluate the length effect of the lateral chain of alkyl-aromatic hydrocarbons on the soot formation tendency. Chosen alkyl aromatics are toluene [5], *n*-butyl-benzene (BBZ) and *n*-heptyl-benzene (HBZ) [5]. The soot formation tendency was characterized under engine conditions by measuring the soot induction delay time (τ_{ind}), the soot growth rate constant (k_f) and the soot yield (Y) at constant carbon atoms concentration. The effect of the

oxygen content on these parameters was investigated through pyrolysis and two equivalence ratios (ϕ), 18 and 5.

Experimental Setup

Experiments on soot formation from alkyl-aromatic hydrocarbons were conducted in a heated stainless steel shock-tube (7.15 m total length, 52 mm in internal diameter). The last part was equipped with four piezoelectric pressure transducers (with a well-know space between them) mounted flush with the internal surface of the shock tube. The last one was 15 mm before the shock tube end wall. In this work, the observation time was around 2 ms for a driven section 5.15 m long. In the same plane as the last transducer, two fused silica windows (9 mm optical diameter and 6 mm thickness) were mounted. Soot formation was monitored by the attenuation of a He-Ne laser beam (632.8 nm) via a photomultiplier equipped with an interferential filter (633 \pm 2 nm). In order to suppress multiple reflections of light, the driven section was blackened near the measurement section. A scheme of the experimental setup is given in figure 1.

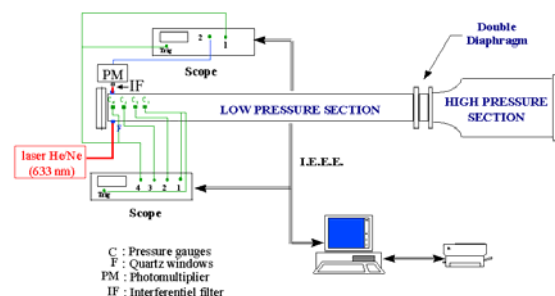


Fig. 1: Scheme of the experimental setup

Experiments with toluene were carried out at room temperature while experiments with BBZ and HBZ, due

* Corresponding author: paillard@cnrs-orleans.fr

to their low vapour pressure, were conducted at 363 K and 403 K, respectively. Reflected shock parameters (P_5 and T_5), at which soot formation is studied, were calculated using the classical procedure [9].

The hydrocarbon/oxygen mixtures were highly diluted in argon. The high pressure gas used for experiments was helium. The liquid hydrocarbons were vaporized in a trace-heated 30 L mixing tank, into which argon and, if needed, oxygen were introduced. To ensure a homogeneous mixture, the magnetic fan was then switched on for no more than half an hour to avoid slow degradation of the mixture in case of the heating of the experimental setup. The concentration in carbon atoms was kept constant around an average value of 10^{18} atoms.cm⁻³ for each mixture. Experimental conditions are given in the Table 1.

	T_5 (K)	P_5 (kPa)	$[C]$ at./cm ³
Toluene [5]	1300-2600	1000-1790	$(1.5-2.3) \cdot 10^{+18}$
BBZ	1465-2675	1090-1690	$(1.7-2.6) \cdot 10^{+18}$
HBZ [5]	1410-2325	640-1120	$(1.4-2.6) \cdot 10^{+18}$

Table 1: Experimental conditions obtained behind reflected shock wave.

Results and Discussion

Determination of the experimental parameters

Soot formation parameters (τ_{ind} , k_f and Y) are deduced from the soot volume fraction signal as it is visible in Figure 2.

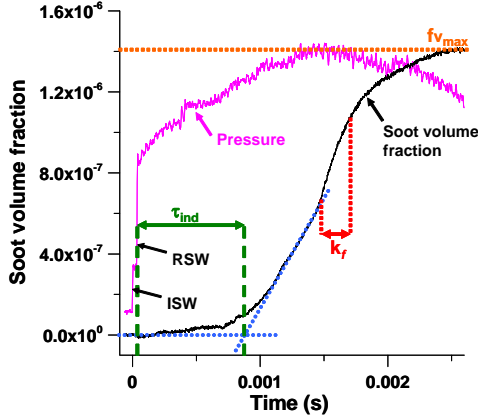


Fig. 2: Soot volume fraction coupled with last pressure transducer signals versus time for a 0.4 % *n*-butylbenzene / 99.6 % argon mixture ($T_5 = 1615$ K, $P_5 = 1120$ kPa). ISW: incident shock wave; RSW: reflected shock wave.

From this figure, one can see that τ_{ind} can be represented by the time interval between the moment at which the gas mixture is heated by the reflected shock wave and the moment at which soot particles appear. After the inflection point of the soot volume fraction profile, during the period where a linear growth can be observed (fig. 2), one can consider that this growth is only due to surface reactions with molecules from the gaseous phase (growth by agglomeration and coagulation of particles is neglected). This period can be

described by a first order rate law where fv is the soot volume fraction:

$$\frac{df_v}{dt} = k_f (fv_{max} - fv) \quad (1)$$

At the end of the growth period, the soot volume fraction profile reaches a maximum and constant value (fv_{max}). The soot yield is defined as the carbon concentration present as soot in relation to the initial carbon concentration:

$$Y = \frac{[C]_{soot}}{[C]_{initial}} \quad (2)$$

The initial carbon concentration is easily deduced from the initial fuel concentration behind the reflected shock wave. The carbon concentration in soot is deduced using the Graham's model [10]:

$$[C]_{soot} = \frac{N_{av} \rho \lambda}{72 \pi d E(m)} \ln \left(\frac{I_0}{I} \right) \quad (3)$$

The maximum and constant value reached by the soot volume fraction (fv_{max}) after the period of growth is used to obtain the soot yield. Literature provides different value for the soot refractive index ($E(m)$) and soot density (ρ). For comparison with the literature data, we choose to use the soot refractive index provided by Lee and Tien [11] and $\rho = 1.86$ g/cm³.

The evolution of the soot yield versus temperature follows a bell-shaped curve [4-6]. In order to describe the evolution of Y versus temperature, the following expression is applied [12]:

$$Y = Y_{max} \cdot \exp \left(-Q \left[\frac{T_m - T}{T} \right]^2 \right) \quad (4)$$

With Y_{max} , the maximum soot yield; T_m , the optimal temperature of soot formation (where the soot yield is maximum) and Q , a correlation factor. During our experiments, for temperature higher than T_m , a second growth stage of the soot volume fraction profile, following the period of first order growth, can be observed. This behaviour was already observed by Kellerer *et al.* for benzene and toluene [13]. In such case, the value of fv_{max} , used for the determination of Y , was determined from this second maximum of the soot volume fraction signal.

Soot Induction delay time

Figure 3 shows the evolution of the soot induction delay time versus temperature for toluene, BBZ and HBZ pyrolysis. As it can be seen from this figure, τ_{ind} decreases exponentially as the temperature increases whereas τ_{ind} increases with the length of the lateral

chain. For example, at 2000 K, τ_{ind} is of 35 μs for toluene, 45 μs and 56 μs for BBZ and HBZ, respectively. Plotting τ_{ind} at 2000 K versus the number of carbon of the lateral chain (n_{CLC}) lead to the following expression established for a carbon atoms of 2×10^{18} per cm^3 :

$$\tau_{\text{ind @ 2000K}} (\mu\text{s}) = \tau_{\text{toluene @ 2000K}} \cdot n_{\text{CLC}}^{0.25} \quad (5)$$

However, this expression does not apply to benzene since it has longer delay than toluene for similar conditions [4, 13].

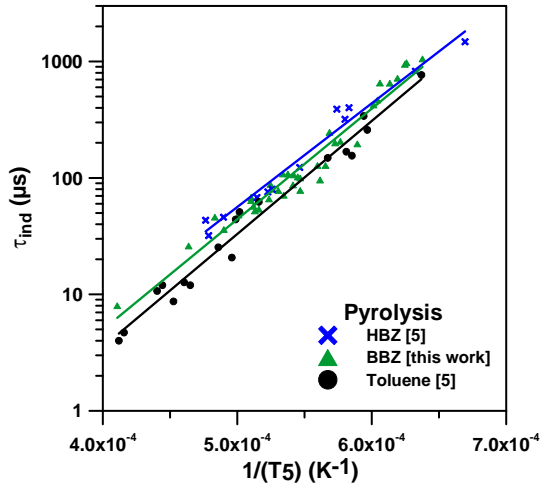


Fig. 3: Soot induction delay time versus temperature inverse for toluene [5], *n*-butyl-benzene (this work) and *n*-heptyl-benzene [5] pyrolysis in similar conditions (see table 1).

The aromatic group is thermally stable and one of the most important soot precursor [14]. It has been already observed that τ_{ind} for aromatic compounds are significantly shorter than τ_{ind} for paraffin [5-6] or naphthene [5]. Moreover, for toluene pyrolysis, τ_{ind} decreases as the fuel concentration increases [12]. Thus, since the carbon atom concentration was kept constant, the behavior observed on fig. 3 can be due to the ratio between the number of carbon atoms from the lateral chain and the number of carbon atoms from the aromatic group ($n_{\text{CLC}}/n_{\text{CA}}$).

The increase of the lateral chain seems also reduces the activation energy: 186 kJ/mol for toluene, 182 kJ/mol for BBZ and 170 kJ/mol for HBZ. This reduction is not very important and a constant value of 178 ± 8 kJ/mol for this kind of hydrocarbon can be adopted.

Using all the data of the figure 3, a correlation between soot induction delay time, temperature and number of carbon atoms of the lateral chain can be derived in the temperature range of 1600-2500 K and at $[C] = 2 \times 10^{18}$ C atoms/ cm^3 :

$$\tau_{\text{ind}} (\mu\text{s}) = 6.10^{-4} [n_{\text{CLC}}]^{0.25} \cdot \exp\left(\frac{21760}{T_5 (\text{K})}\right) \quad (6)$$

Due the presence of the aromatic group, the influence of the oxygen content on the delay is not very important. This effect was visible in [15] for toluene and in [5-6] for HBZ. With these two hydrocarbons, a small decrease of τ_{ind} was observed when oxygen was added. Soot were not detected at $\phi=5$ for HBZ which was the alkyl aromatic with the higher $n_{\text{CLC}}/n_{\text{CA}}$ studied. In the case of the BBZ (figure 4), the oxygen addition had no effect when $\phi=18$ and τ_{ind} was slightly increased at $\phi=5$. This kind of result, when τ_{ind} is increased by oxygen addition, have been already seen for toluene in shock tube [16].

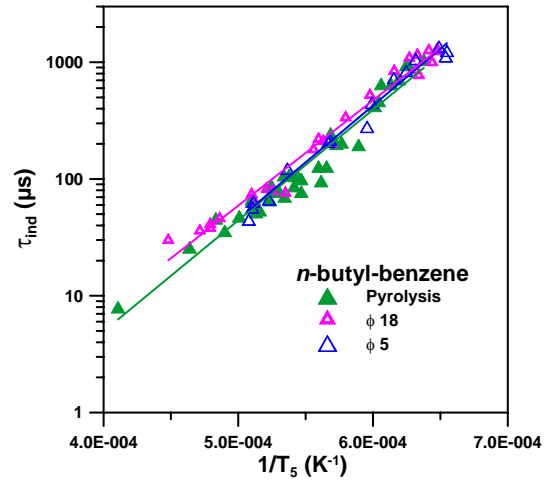


Fig. 4: Effect of oxygen content on *n*-butyl-benzene soot induction delay time versus temperature inverse.

Soot growth rate constant

The evolution of the soot growth rate constant with the temperature is visible on the fig. 5. As it can be seen from this figure, k_f increases with the n_{CLC} for temperature below 1900 K. However, k_f increases with the temperature on all the temperature range with toluene and BBZ whereas a decrease of k_f is observed for temperature higher than 1800 K in the case of HBZ. Using data from the literature, it is visible that the evolution with temperature of the soot growth rate constant is dependant of the structure of the hydrocarbon. Indeed, a similar behavior was observed with toluene [5], BBZ (this work), benzene [4, 17] and 1-methyl-naphthalene [5] pyrolysis. Concerning, HBZ, a behavior similar to aliphatic compounds (acetylene [17], ethylene and *n*-hexane [4], *n*-hexadecane and decahydro-naphthalene [18]) can be observed. Such behavior is certainly due to the $n_{\text{CLC}}/n_{\text{CA}}$ ratio.

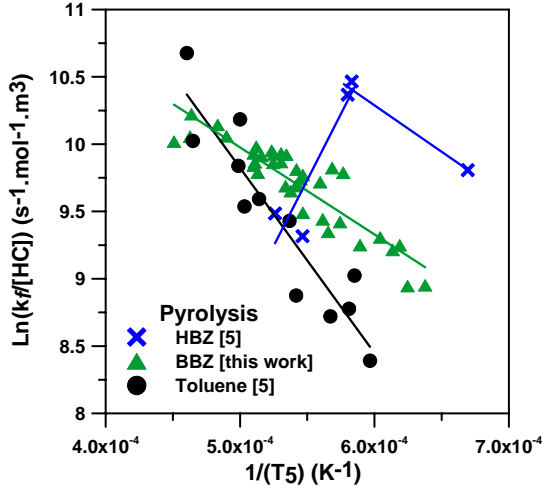


Fig. 5: Soot growth rate constant versus temperature for toluene [6], *n*-butyl-benzene and *n*-heptyl-benzene [6] pyrolysis in similar conditions (see table 1).

Concerning the evolution of k_f with the temperature in presence of oxygen, as far as we know, there is no data in shock tube available in the literature. This paper gives the opportunity to see such evolution on figure 6 for the BBZ, in pyrolysis and at $\phi=18$ and 5. It appears from figure 6 that the oxygen addition leads to a decrease of k_f at temperature above 1900 K. The comparison of results obtained in pyrolysis and at $\phi=18$ exhibits a similar behavior: activation energy are of 54 and 56 $\text{kJ}\cdot\text{mol}^{-1}$, respectively. However, a decrease of k_f by around 30 % can be observed when oxygen is added. Results obtained at $\phi=5$ show a different evolution (activation energy = 26 $\text{kJ}\cdot\text{mol}^{-1}$). This is certainly due to the small amount of soot formed in these conditions, leading to an imprecise determination of the soot growth rate constant.

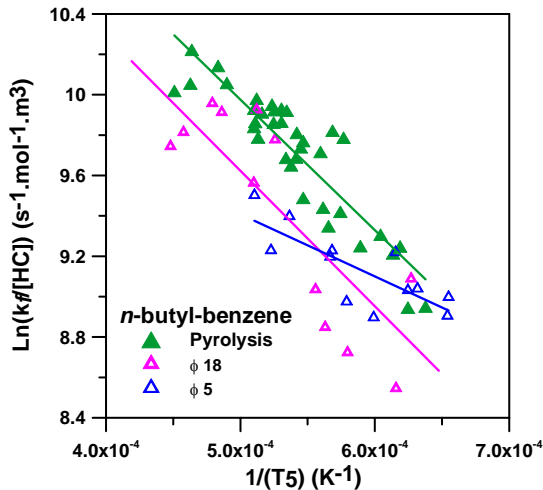


Fig. 6: Effect of oxygen content on soot growth rate constant versus temperature for *n*-butyl-benzene.

Soot yield

Figure 7 shows the evolution of the soot yield versus temperature for the considered hydrocarbons in

pyrolysis. As it can be seen from this figure, the soot yield and the optimal temperature of soot formation decrease with the number of carbon in the lateral chain. It is well known that, in similar conditions, aromatics give a value of Y_{\max} significantly higher than aliphatics (for example by comparing benzene and *n*-hexane [4]). Consequently, the decrease of Y_{\max} with $n_{\text{CLC}}/n_{\text{CA}}$ in the present study is certainly due to the $n_{\text{CLC}}/n_{\text{CA}}$ ratio. In other words, the more carbon atoms are proportionally present in the aromatic group of an alkyl-aromatic fuel, the more the maximum soot yield is high.

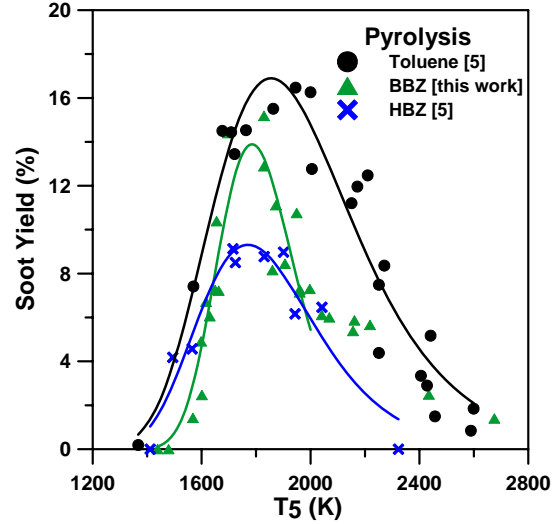


Fig. 7: Soot yield versus temperature for toluene [6], *n*-butyl-benzene (this work) and *n*-heptyl-benzene [6] pyrolysis in similar conditions (see table 1).

The threshold temperature for soot apparition however, does not seem to be linked with the number of carbon atom of the lateral chain.

Oxygen addition decreases strongly the soot yield. Results obtained for toluene and HBZ at equivalence ratios of 18 and 5 are visible in [5]. For the BBZ, the inhibiting effect of oxygen on the soot yield is presented on figure 8. As it can be seen, Y_{\max} is close to 14 % in pyrolysis condition and close to 6 and 2.9 % at $\phi=18$ and 5, respectively. These important reductions of the soot yield when oxygen is added are the result of carbon consumption from gaseous phase and from soot surface by heterogenous oxidation which lead to the reduction of the soot volume fraction profile.

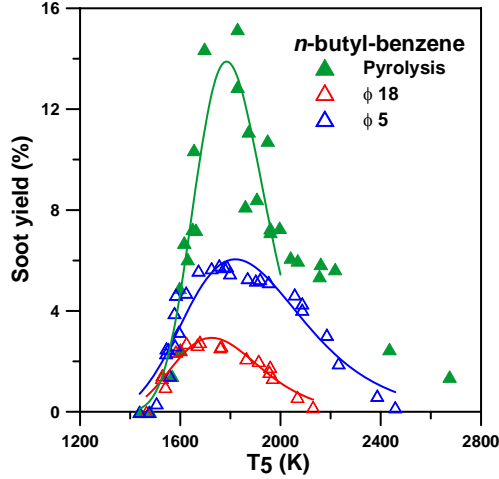


Fig. 8: Effect of oxygen content on *n*-butyl-benzene's soot yield.

Using result given by the relation (4), applied to the data of figures 7 and 8 (represented with continuous line) and soot yield data of toluene and HBZ from [5], it is possible to represent the evolution of Y_{\max} with n_{CLC} for different equivalence ratios (fig. 9). From figure 9, one can see that, at constant carbon atoms concentration, the maximum soot yield decreases with the number of carbon of the lateral chain for each investigated condition. As oxygen is added to the mixture, the same trend is observed for the variation of the maximum soot yield versus n_{CLC} .

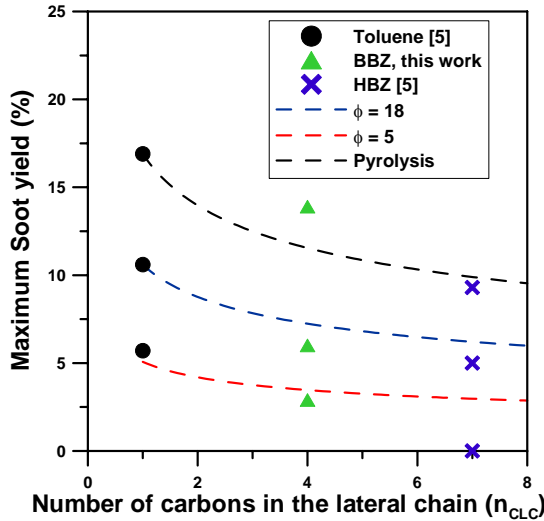


Fig. 9: Evolution of the maximum soot yield for alkyl-aromatic fuels versus the number of carbon of the lateral chain and the equivalence ratio.

For each studied fuel, the decrease of the maximum soot yield as oxygen is added to the mixture can be derived, once the maximum soot yield in the pyrolysis conditions is known, according to the following expression:

$$Y_{\max, \Phi} = Y_{\max, \text{pyrolysis}} \cdot \left[1 - \left(\frac{2.5}{\Phi} \right)^{0.5} \right] \quad (7)$$

From figure 9, one can see that the maximum soot yield obtained, for pyrolysis conditions, can be expressed as a function of the number of the carbon atoms of the lateral chain. From this result, the following expression can be derived which allows the prediction of the maximum soot yield of alkyl-aromatics based on the maximum soot yield of toluene and on n_{CLC} :

$$y_{\max, \text{alkyl}} = y_{\max, \text{toluene}} \cdot (n_{\text{CLC}})^{-0.275} \quad (8)$$

Using both expressions (7) and (8), one can derive the maximum soot yield both for pyrolysis and oxidation conditions for alkyl-aromatics with an average error of 15 %. One has to keep in mind that these expressions have been derived for a carbon atoms concentration of $2 \times 10^{+18} \text{ atoms.cm}^{-3}$.

From fig. 10, one can see that T_m decreases by following a power law with n_{CLC} in pyrolysis conditions. The following expression was derived using the experimental data:

$$T_{\text{opt}} (\text{K}) = 1855 \cdot (n_{\text{CLC}})^{-0.0242} \quad (9)$$

As for the evolution of τ_{ind} with n_{CLC} , these rules (decrease of Y_{\max} and T_m with n_{CLC}) can not be derived for benzene. Indeed, Y_{\max} for toluene is higher than the benzene's one whereas T_m is lower, in similar pyrolysis conditions [19].

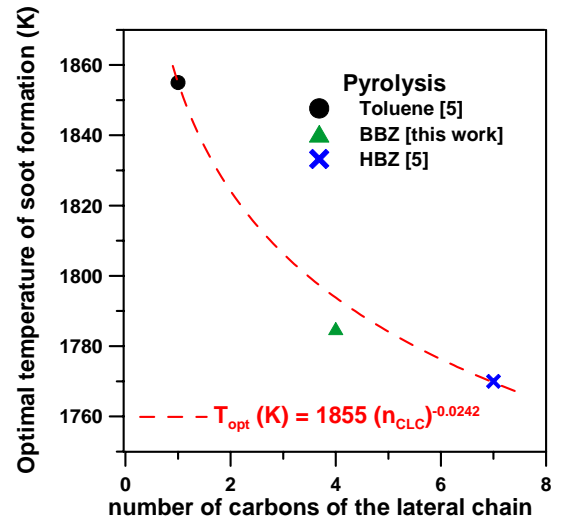


Fig. 10: Evolution of the optimal temperature of soot formation with the number of carbon of the lateral chain for the pyrolysis of alkyl-monoaromatic fuels.

Conclusions

The study of soot particles formation in shock tube from alkyl aromatic fuels at constant carbon atoms concentration and at three equivalence ratios have showed that soot formation parameters (soot induction delay time, soot growth rate constant and soot yield) are dependent on the number of carbon of the lateral chain:

- τ_{ind} increases with the length of the lateral chain and a correlation expression of the soot induction

delay time with the temperature and the number of carbon atoms of the lateral chain was derived with a significant correlation coefficient.

- The soot growth rate constant increases with the temperature for mono-aromatic hydrocarbon. However, for *n*-heptyl-benzene which presents a long lateral chain and a high n_{CLC}/n_{CA} ratio, the evolution of k_f is similar to those already observed in the literature for aliphatic fuels.
- Maximum soot yield is strongly dependant of the number of carbon of the lateral chain and the equivalence ratio. A correlation expression allowing to link-up these parameters was obtained from experimental results.

The overall result of this study is the following: it is possible to estimate roughly some soot formation parameters (namely soot induction delay time and soot yield) for alkyl-aromatic fuels as a function of the number of carbon of the lateral chain and the equivalence ratio.

Acknowledgements

Authors want to thank TOTAL France for the financial support.

Nomenclature

BBZ	<i>n</i> -butyl-benzene
HBZ	<i>n</i> -heptyl-benzene
n_{CLC}/n_{CA}	ratio between the number of carbon atoms from the lateral chain and the number of carbon atoms from the aromatic group
n_{CLC}	number of carbon in the lateral chain
P_5	reflected shock pressure (kPa)
T_5	reflected shock temperature (K)
T_m	optimal temperature of soot formation (K)
τ_{ind}	soot induction delay time (μs)
k_f	soot growth rate constant (s^{-1})
Y	soot yield
Y_{max}	maximum soot yield
$[C]_{soot}$	concentration of carbon atoms in soot particles formed ($atoms/cm^3$)
$[C]_{initial}$	initial concentration of carbon atoms in the fuel ($atoms/cm^3$)
f_v	soot volume fraction
N_{av}	Avogadro constant
ρ	soot density
λ	wavelength (632.8 nm in this study)
l	length of the optical path (52 mm in this study)
I_0	intensity of incident light
I	intensity of transmitted light
$E(m)$	complex refractive index (m) function
ϕ	equivalence ratio

References

- [1] S. VEDAL. *J. of the Air and Waste Management Association* 47 (1997), 551-581.
- [2] B. GRANUM, M. LØVICK. *Toxicological Sciences* 65 (2002), 7-17.

- [3] M.Z. JACOBSON. *J. of Geophysical Research* (2002), vol. 107, D19, 4410, ACH16-1- ACH16-22.
- [4] S.T. BAUERLE, Y. KARASEVICH, S.T. SLAVOV, D. TANKE, M. TAPPE, T.H. THIENEL, H. Gg. WAGNER. *Proc. of the 25th Symp. (Int.) on Comb., The Comb. Inst.* (1994), 627-634.
- [5] F. DOUCE, N. DJEBAÏLI-CHAUMEIX, C.-E. PAILLARD, C. CLINARD, J.-N. ROUZAUD. *Proc. of the 28th Symp. (Int.) on Comb., The Comb. Inst.* (2000), 2523-2529.
- [6] O. MATHIEU, N. DJEBAÏLI-CHAUMEIX, C.-E. PAILLARD. *Proc. of the European Combustion Meeting* 2005.
- [7] Private communication, TOTAL France.
- [8] P. DAGAUT, M. CATHONNET. *Progress in Energy and Comb. Sciences* (2006), 48-92.
- [9] C.-E. PAILLARD, S. YOUSSEFI, G. DUPRE. *Prog. Astronaut. Aeronaut.* 105 (1986), 394.
- [10] S.C. GRAHAM, J.B. HOMER, J.L.J. ROSENFELD. *Proc. R. Soc. Lond. A.* 344, 259-285.
- [11] S.C. LEE, C.L. TIEN. *Proc. of the 18th Symp. (Int.) on Comb., The Comb. Inst.* (1981), 1159-1166.
- [12] O. MATHIEU, G. FRACHE, N. DJEBAÏLI-CHAUMEIX, C.-E. PAILLARD, G. KRIER, J.-F. MULLER, F. DOUCE, P. MANUELLI. *Proc. of the 31st Symp. (Int.) on Comb., The Comb. Inst.* (2006), *In press*.
- [13] H. KELLERER, R. KOCH, S. WITTIG. *Comb. and Flame* 120 (2000), 188-199.
- [14] M. FRENKLACH, D.W. CLARY, W.C. GARDINER Jr., S.E. STEIN. *Proc. of the 21st Symp. (Int.) on Comb., The Comb. Institute*, 1986, 1067-1076.
- [15] F. DOUCE, N. DJEBAÏLI-CHAUMEIX, C.-E. PAILLARD, C. CLINARD, J.-N. ROUZAUD. *Proc. of the 4th Int. Conf. on Internal Combustion Engine: Experiments and Modeling*, (G. Peritore ed.), Puzzuoli, Italy (1999) 251-258.
- [16] A. ALEXIOU, A. WILLIAMS. *Comb. and Flame* 104 (1996), 51-65.
- [17] V.G. KNORRE, D. TANKE, T.H. THIENEL, H. Gg. WAGNER. *Proc. of the 26th Symp. (Int.) on Comb., The Comb. Inst.* (1996), 2303-2310.
- [18] F. DOUCE. Ph.D. Thesis, Université d'Orléans, France, 2000.
- [19] M. FRENKLACH, M.K. RAMACHANDRA, R.A. MATULA. *Proc. of the 20th Symp. (Int.) on Comb., The Comb. Institute*, 1984, 871-878.